Proceedings of the 3rd International Conference on Green Energy, Environment and Sustainable Development (GEESD2022), X. Zhang et al. (Eds.)

doi:10.3233/ATDE220397

Study on Hydrate Formation in Deep-Water Gas Well Intervention Operation

Heng WANG[a], Huan DIAO[a], Tan XIAO[a], Donglei JIANG[a], Yi YU[a], Zhandong LI[b,c,d], Bicheng GAN[c,d,1] and Fabao ZOU[c]

[a] *Hainan Branch of CNOOC Ltd., Haikou 570311, Hainan, China*
[b] *Heilongjiang Key Laboratory of Gas Hydrate Efficient Development, Daqing 163318, Heilongjiang, China*
[c] *College of Offshore Oil & Gas Engineering, Northeast Petroleum University, Daqing 163318, Heilongjiang, China*
[d] *Sanya Offshore Oil & Gas Research Institute, Northeast Petroleum University, Sanya 572024, Hainan, China*

Abstract. In the development of deepwater high temperature and pressure gas wells, frequent intervention operations are required. Wellbores near the seabed have the risk of producing massive hydrates and plugging the wellbore. Based on the non-steady state model, a temperature-pressure coupling model of deepwater gas well intervention was established, and a physical simulation experiment of hydrate formation under deepwater gas well intervention was carried out by using the self-developed hydrate deposition simulation reaction device. Intervention operation of deepwater high temperature and high pressure gas wells. With reference to the test data of a real well in the South China Sea, the hydrate formation rate was analyzed under the influence of different production rates, running speed and tool size, temperature and pressure distribution of deepwater gas wells. The operation rules of deepwater gas well intervention and the formation rules of hydrates are obtained. Simulation prediction results can be used to predict the timing and location of hydrate plugging under intervention operations..

Keywords. Deep-water gas well, intervention operation, lowering tools, hydrate formation, temperature-pressure coupling, high temperature and pressure

1. Introduction

Deep water gas well face various risks of hydrate formation and plugging the wellbore from drilling to production [1-2]. Therefore, it is particularly important to address the problem of flow assurance caused by hydrates in deep-water gas wells. Hydrate flow assurance is to prevent the formation of a hydrate layer on the wellbore that hinders fluid migration in gas wells. Compared with other types of reservoirs, deep-water gas reservoirs have a higher probability of generating hydrates in the wellbore to block the wellbore [3-6]. As shown in the table, once the wellbore is blocked by hydrate in the wellbore, it will directly affect the operation progress and cause great economic losses. As a result, one of the crucial research projects on the secure and effective development

[1] Corresponding Author, Bicheng GAN, College of Offshore Oil & Gas Engineering; Sanya Offshore Oil & Gas Research Institute, Northeast Petroleum University, Northeast Petroleum University, Daqing 163318, Heilongjiang, China; Email: gbicheng@foxmail.com.

of deep-water gas wells both domestically and internationally is the flow assurance of hydrate in deep-water gas wells.

The flow assurance issue brought on by hydrate blockage has been the subject of several theoretical and experimental investigations by academics both domestically and abroad, the majority of which concentrate on oil and gas collection and transportation pipelines [7], throttle valves [8] and oil-based systems in the rich liquid phase [7-9] and water-based systems [10]. The study of gas-dominated hydrate flow assurance in deepwater gas wells, however, came much later [11]. Many variables, including the kind of transport medium in the pipe, the flow velocity in the pipe, the pattern of the flow in the pipe, and the degree of subcooling, have a significant impact on the formation process of the hydrate flow barrier in deepwater gas wells [12]. Deep-water gas wells currently face several issues due to the lack of a good understanding of the hydrate flow impediments created by varied operating conditions. This makes it difficult to identify and avoid hydrate formation sites in deep-water gas wells.

2. Wellbore Temperature-Pressure Coupling Model under Intervention Operation

Deep-water gas well intervention operation models are currently lacking, and it is challenging to characterize them quantitatively. The steady-state model is primarily used in the calculation and analysis of the temperature and pressure field of deep-water gas wells, but the intervention operation is a transient issue. Large errors will result from using the steady-state model or simplifying it to a quasi-transient model. Research on the coupled model of temperature and pressure in deep-water oil and gas wells has been extensive both domestically and internationally, but transient flow factors like formation inflow, wellbore flow law, heat transfer changes of intervention tools, and gradient changes in frictional resistance changes have only rarely been taken into account. An accurate understanding of the temperature, pressure, and flow state of the wellbore under operation cannot establish a temperature-pressure coupling model under intervention operation. Based on the problem, the wellbore structure of the deep-water gas well is divided into two parts: between the wellbore and the formation and between the wellbore and the seawater, and the corresponding temperature-pressure coupling models are constructed respectively. Taking the fluid micro-element with length Δz as the research object, the unsteady heat transfer models of the seawater section above the midline and the formation section below the midline are established respectively.

The fluid element's energy change is equal to the energy difference between the system's incoming and outgoing energy.

$$dQ=H(z+\Delta z)-H(z)+\frac{1}{2}mv^2(z+\Delta z)-\frac{1}{2}mv^2(z)+mgz+mg(z+\Delta z sin\theta)-mgz \tag{1}$$

In the formula, dQ is the change of the energy of the micro-element; $H(z+\Delta z)$ and $H(z)$ are the enthalpy of the fluid; $\frac{1}{2}mv^2(z)$ and $\frac{1}{2}mv^2(z+\Delta z)$ are the kinetic energy term of the fluid; mgz and $mg(z+\Delta z sin\theta)$ are the positional potential energy of the fluid in the wellbore. The transient heat transfer model of the fluid in the wellbore can be obtained by writing the above equation in the differential form:

$$\frac{\partial^2 T}{\partial r^2}+\frac{1}{r}\frac{\partial T}{\partial r}=\frac{\partial T}{\partial r} \tag{2}$$

The fluid in the wellbore is subject to unsteady heat transfer to the formation in the formation section below the mud line, and the only source of heat loss is radial heat transfer. The calculation formula for the temperature of the wellbore fluid formation section can be obtained:

$$\frac{dT}{dz}=\frac{1}{C_{pm}}\frac{dh}{dz}+C_j\frac{dP}{dz} \tag{3}$$

In the formula, C_{pm} is the specific heat capacity of the fluid at constant pressure, J/(kg °C); C_j is the Joule-Thompson coefficient, °C/Pa. Similar to the temperature of the fluid in the wellbore below the mud line, the temperature model of the heat transfer model in the seawater section above the mud line was derived. The wellbore fluid's temperature and the equation for heat transfer from the wellbore fluid to the wellbore are as follows:

$$\frac{dQ}{dz}=-\frac{2\pi r_{ro}U_{to2}}{W}(T_f-T_{sea}) \tag{4}$$

Bringing into the energy conservation formula, the temperature change formula in the wellbore is:

$$\frac{dT}{dz}=\frac{(T_{sea}-T_f)(2\pi r_{co}U_{to2})}{C_{pm}W}-\frac{g\sin\theta}{C_{pm}}+C_j\frac{dP}{dz}-\frac{vdv}{C_{pm}dz} \tag{5}$$

where r_{co} is the outer radius of the riser, m; U_{to2} is the total heat transfer coefficient of the seawater section, W/(m^2 °C); the seawater temperature model a_T is calculated using the Leviticus statistical model of world ocean temperature data. It has been demonstrated in the lab and in the field that a variety of factors influence how the temperature and pressure profile change in the wellbore of high temperature and pressure gas wells [10]. Prior to production, the fluid inside the wellbore exists as a static gas and liquid column with a temperature that is similar to the surrounding air. The fluid at the bottom of the well mixes with the fluid at the wellhead once it has been put into production. A two-phase mass flow of gas and liquid is present inside the wellbore. As the fluid continues to lift during the production process and continuously releases heat to the formation and seawater, the gas and liquid in the formation continue to enter the wellbore. After a period of the blowout, the fluid in the wellbore gradually flows stably [11-12]. Based on the above phenomenon, the two-phase transient pressure calculation formula during the tool running process during well clearance and blowout is constructed:

$$-\frac{dP}{dz}=\rho_{cen}g\sin\theta+\frac{f_{cen}v_g^2\rho_{cen}}{2d}+\rho_{cen}v_g\frac{dv_g}{dz} \tag{6}$$

Among them, v_g can be calculated as:

$$v_g=C_ov_m+v_{rg} \tag{7}$$

Among them, C_o is the gas distribution coefficient; d is the inner diameter of the tubing, m; v_g is the gas velocity; ρ_{cen} is the fluid density at the center of the string, kg/m^3; v_{rg} is the gas slip velocity, m/s. Equation (10), which states that the intervention tool alters the wellbore's fluid flow section, explains why the fluid flow rates in the tool's

upper and lower sections are inconsistent. As the drilling tool is lowered and raised, the flow rate of the fluid in the wellbore will change. The fluid flow rate in the wellbore changes depending on how quickly the intervention tool is lowered, to use an example using a pipe string of a specific size:

$$v_g' = \frac{\frac{W}{\rho_g} B_g + v_{sp}\pi\left(\frac{d_s}{2}\right)^2}{2\left[\left(\frac{d}{2}\right)^2 - \left(\frac{d_s}{2}\right)^2\right]} \tag{8}$$

When the intervention job tool is stopped, $v_{sp} = 0$. Among them, v_{sp} is the running speed of the tool, m/s; d is the inner diameter of the tubing, m; d_s is the diameter of the intervention tool, m. Therefore, the pressure on the working section of the intervention operation can be calculated according to the following formula:

3. Physical Simulation Experiment of Hydrate Formation

3.1. Experimental Materials

Distilled water and 99.9 percent pure methane gas made up the experimental components. Additionally, a laboratory distilled water preparation machine was used to create the distilled water.

3.2. Experimental Setup

The experimental apparatus is a self-designed hydrate deposition simulation reaction device, which includes a sample rod lifting system, a liquid injection system, a gas injection system, a back pressure system, a pressure-temperature displacement measurement system, a data acquisition system, and a visual reaction system. The system composition is shown in Figure 1. The liquid injection system includes a liquid displacement pump, distilled water, and a liquid injection pipeline. The gas injection system includes a methane gas cylinder, a gas booster pump, and a gas injection pipeline. The backpressure system includes a safety valve, a back pressure container, and a gas flow meter. The displacement measurement system is composed of a pressure sensor, a temperature sensor, and a displacement sensor; the data acquisition system records and saves the collected pressure, temperature and displacement data in the computer, and the acquisition time interval is the 20 s; the temperature control system realizes the experimental environment temperature through the thermostat. Control; the automatic lifting system of the sample rod is composed of a turbine worm reducer, a stepping motor, and a ball screw; the visual reaction system is composed of a visual reaction kettle and an electron microscope at the bottom and sides. The main device in this experiment is a visual reaction kettle. The visual reaction kettle is equipped with a pressure sensor (range 40 MPa, accuracy 0.25%), temperature sensor (temperature range -50℃-200℃, accuracy ±0.1℃), displacement sensor (stroke 0-175 mm, linear accuracy 0.05% FS), the kettle body is made of sapphire glass, the volume is 135m L, the maximum working pressure is 30MPa, the working temperature range is -10℃-50℃, the temperature fluctuation is ±0.5℃, and the inner side of the kettle is Φ35×140.5 mm. The upper and lower covers of the reactor are detachable, and the lower cover is provided with a visual

window, which is convenient for real-time observation of the hydrate formation in the reactor from the bottom end face.

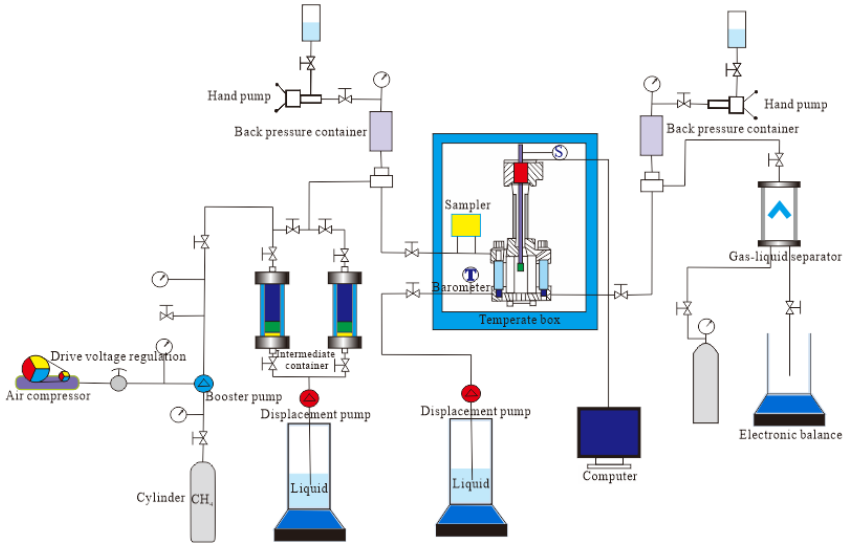

Figure 1. Experimental flow chart.

3.3 Experimental Steps

The air tightness test of the experimental device is performed prior to the experiment in order to guarantee the experiment's accuracy and safety. The main experimental steps are:

- Set the experimental temperature through the incubator temperature control system. The temperature in the reaction kettle should be consistent with the temperature in the incubator;
- Open the outlet valve of the visual reactor so that the outlet interface is connected to the backpressure system, and set the backpressure of the backpressure system to the initial pressure of the experiment;
- Open the gas injection valve of the visual reactor, vent the end for some time, so that the gas in the pipeline is methane gas, and slowly inject gas into the gas injection port of the visual reactor through the gas booster pump to slowly increase the pressure in the kettle until after reaching the initial pressure of the experiment, stop the gas injection and let it stand for 30min;
- When the temperature in the visual reactor is the same as the set temperature of the incubator, turn on the constant speed and constant pressure pump to inject methane gas into the visual reactor at the preset gas injection rate. Then, open the liquid injection valve of the visual reactor to the injection speed to inject distilled water through the visual reactor's liquid injection interface;
- Utilize the data acquisition system to capture the data in real-time, use the electron microscope to observe in real-time, and take pictures every five minutes to document the distribution and formation of hydrates;

- Adjust the backpressure valve to evacuate the methane gas in the kettle so that the pressure in the kettle drops to 0, after the temperature and pressure in the reaction kettle are stable for 0.5 to 1 hour, and count the volume of methane gas discharged through the gas flow meter, disassemble the reaction kettle, and react the interior of the kettle and the pipelines were cleaned for the next set of experiments.

4. Results and Discussion

The South China Sea deep-water gas well's parameters are the subject of the experiment. Table 1 displays the particular variables. In the experiment, which examined the formation of hydrates in the wellbore of deep-water high-temperature and high-pressure gas wells under various operating conditions, the determination of the wellbore temperature and pressure field under the intervention operation and the hydrate formation in the pipe string, respectively, were carried out. This was done using the above temperature-pressure coupling calculation model and the experimental scheme of hydrate formation. Create a physical simulation experiment, and using the experimental data and results, analyze how variables like tool running speed, tool size, and gas production affect the formation of hydrate in the pipe string during the intervention operation..

Table 1. Deep-water gas well parameters in the South China Sea.

Bottom hole formation temperature (℃)	**Total heat transfer coefficient of seawater W/(m²•℃)**	**Formation of total heat transfer coefficient W/(m²•℃)**	**Formation thermal conductivity W/(m•℃)**	**Formation thermal diffusivity (m²/s)**	**Well deep (m)**	**Geothermal gradient (℃/100m)**	**Formation heat capacity J/(kg•℃)**
84.83	18	15	2.312	0.00005	3000	2.55	1700
Wellbore size (m)	**The inner diameter of the casing (m)**	**The outer diameter of the casing (m)**	**Gas production 104 (m³/d)**	**The outer diameter of the tubing (m)**	**Oil pipe thermal conductivity W/(m•℃)**	**Thermal conductivity of casing W/(m•℃)**	**Thermal conductiviy y of cement sheath W/(m•℃)**
0.62	0.52	0.54	43	0.1143	40	35	0.8
Gas relative density	**formation pressure (MPa)**	**stratigraphic density (kg/m³)**	**Tubing inner diameter (m)**	**Sea depth (m)**	**Gas viscosity (mPa•s)**	**Gas compressibi -lity**	**Gas volume factor**
0.684	29.473	2400	0.086	1800	0.033	0.0056	0.0025

The wellbore's daily gas production is a significant contributor to the variation in its temperature and pressure field, and the wellbore's temperature and pressure field differ significantly depending on the rate at which gas is produced. According to Figure 2, the tubing's diameter percentage in the running tool size is 1%, and the running speed is 0.5 m/s for the data on wellbore temperature and pressure. Calculate the wellbore temperature and pressure data of 20×104 m^3/d, 40×104 m^3/d, 60×104 m^3/d, and 80×104 m^3/d respectively, and examine how production affects the pressure field and wellbore temperature during the intervention operation. As wellbore production increases, the pressure inside the wellbore gradually rises, the depth of the wellbore increases, and the pressure inside the wellbore gradually decreases. In the early stage of the intervention

tool, the pressure increase in the wellbore is the largest. When the intervention tool is lowered into the bottom hole, the pressure difference is the smallest under the influence of production. The change in production has the greatest impact on the temperature at the mud line and the least impact on the wellhead and bottom hole as production increases and the temperature of the fluid in the wellbore gradually decreases.

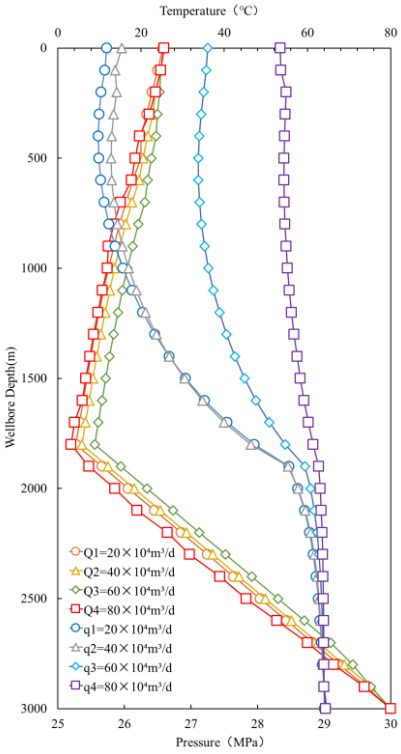

Figure 2. Temperature and pressure profiles in the wellbore under various production conditions

Under the corresponding working conditions, the speed of the lowering tool is controlled, and the gas flow, temperature, and pressure point are adjusted. The rate of hydrate formation was calculated based on the thickness of hydrate formation in the bottom section of the reactor over time. In order to identify the hydrate formation area in the deep-water gas well, Figure 3 displays the curves of the hydrate formation rate in the wellbore along with the distribution of the wellbore under various gas production conditions. The rate of hydrate formation in the wellbore first rises and then falls as the depth of the well increases, peaking at a depth of about 1800 m, and then rapidly falling at a depth of 2000 m below the mud line.The side view and top view of hydrate formation in the wellbore from 0 to 2000 m are shown in Figure 4. The reason is that a significant heat exchange with the seawater takes place when the gas-water two-phase flow moves from the high-temperature and high-pressure gas reservoir through the formation to the seawater layer. It is difficult to produce hydrate at the mud line, though, because of the high temperature of the gas-water two-phase flow there. The temperature of the gas-water two-phase flow rapidly decreases as the heat exchange process continues, gradually satisfying the requirements for the formation of hydrates, and hydrates are

quickly formed in the wellbore. The temperature of the seawater gradually increases to the sea surface temperature as the water depth decreases, and under the influence of heat exchange, the temperature of the gas-water two-phase flow also changes synchronously with the seawater temperature. The formation rate of internal hydrate gradually slowed down to zero.

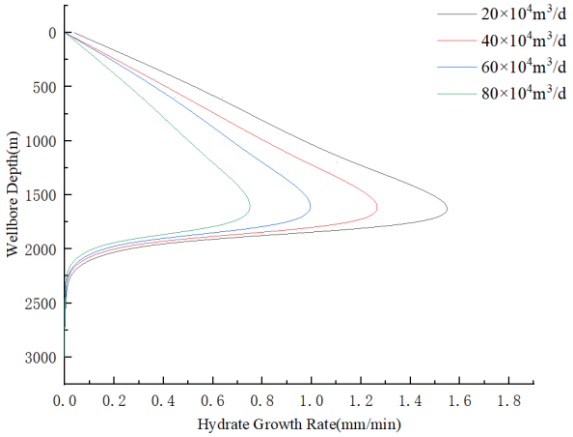

Figure 3. Comparison of hydrate formation rates under different gas production rates.

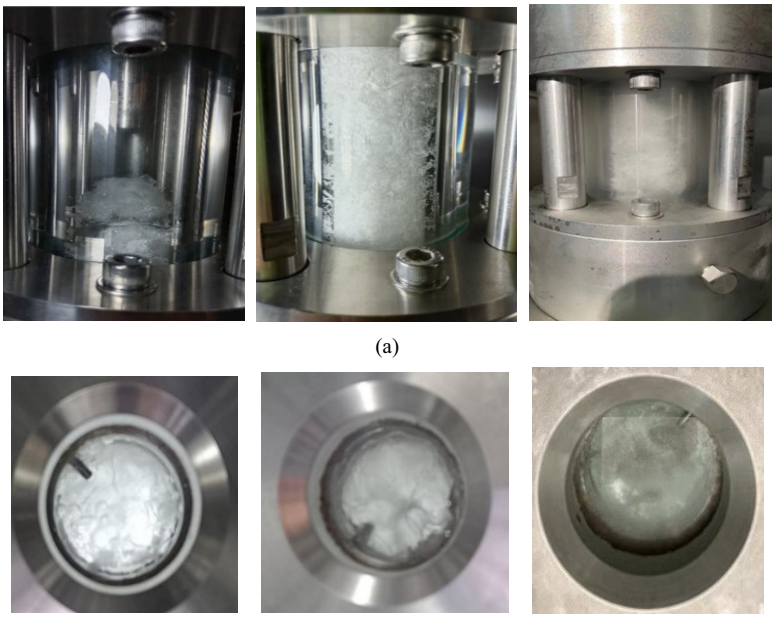

(a)

(b)

Figure 4. Process diagram of hydrate deposition plugging the pipe string.

The running size of the tool, which has a direct impact on the flow distribution of the fluid in the wellbore, is a crucial parameter in the intervention operation. Under the conditions of daily gas production of 40×104 m^3/d and tool running speed of 0.5 m/s, the

percentage of running tool size is calculated as 1%, 25%, 50%, and 75% of wellbore temperature and pressure data, respectively, Figure 5 illustrates wellbore temperature and pressure curves for various tool sizes. The figure shows that the pressure increase in the wellbore is inversely proportional to the size of the running tool. With an increase in running size, the wellbore's temperature rises. The larger the size of the running tool, the higher the temperature at the inflection point. The change in the tool size has a greater impact on the temperature in the wellbore at the mud line.

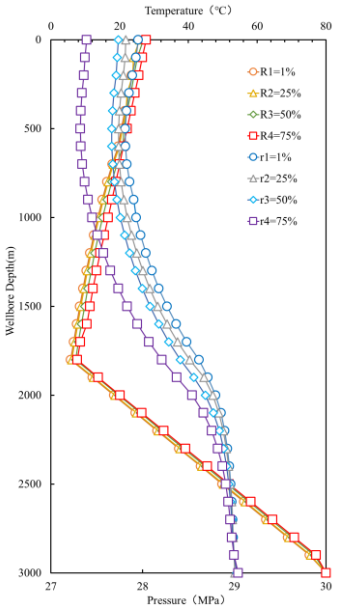

Figure 5. Profile of wellbore pressure and temperature for various tool sizes.

The temperature and pressure point are adjusted under the appropriate working conditions, the running tool size is adjusted, and the formation rate of hydrate in deep-water gas wells is calculated under various running tool sizes, as shown in Figure 6. When running tools of different sizes, the relationship between hydrate formation rate and deep-water also follows the law that hydrate formation rate first increases slowly and then decreases rapidly with increasing depth. However, as the running tool size increases, the rate of hydrate formation in the wellbore initially rises and then falls. Before the running tool size percentage reaches 50%, the hydrate generation rate rises with tool size and the percentage of running tool size reaches 50%. At 2000 meters, the formation rate peaks, and as the size of the running tool rises, the rate of hydrate formation in the wellbore declines. The reason is that the size of the running tool increases, which compresses the inner volume of the pipe string. When a specific gas well flow rate is met, the extended range pressure drop of the gas well decreases, the gas well pressure rises, and the rate of gas production rises. The decrease in pressure promotes the formation of hydrate increasing the rate of hydrate formation. However, when the disposition tool exceeds 50%, the gas-water two-phase mixture encounters a sudden decrease in the channel cross-section in the pipe string during the production process of the gas well, so that the pressure gradually decreases, and a throttling effect occurs. In addition, due to the increase of the pipe string, the volume in the gas well decreases, the flow rate of the

gas-water two-phase flow increases, and the ability to carry hydrates are enhanced. Decomposition of the region where the material is generated. The early stage of hydrate formation is accelerated by an increase in pressure in the wellbore caused by volume compression, which in turn encourages hydrate formation. Later, the rate of hydrate formation is reduced by a throttling effect in the wellbore brought on by an increase in running tools to a certain extent.

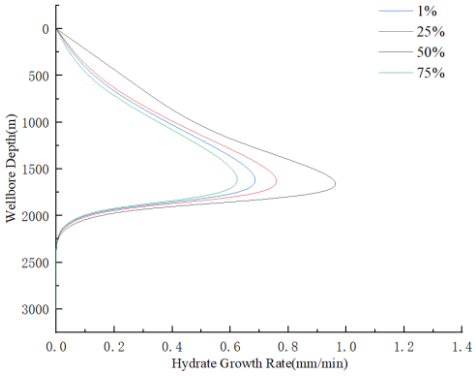

Figure 6. Variation of hydrate formation rate for different tool sizes.

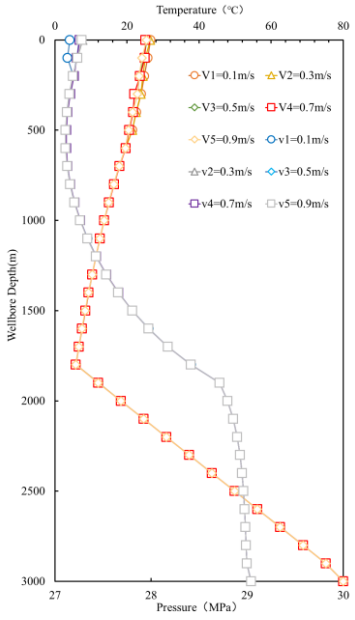

Figure 7. Wellbore pressure and temperature profiles at various speeds of operation.

Figure 7 demonstrates that the wellbore's daily gas production is $40\times10^4 m^3/d$, the running tool's size is 1 percent, and the chosen running speeds are 0.1 m/s, 0.3 m/s, 0.5 m/s, 0.7 m/s, and 0.9 m/s, respectively. Data on wellbore pressure and temperature that were calculated. Although the temperature and pressure in the wellbore do not change significantly under different running speed conditions and are less sensitive to changes

in tool running speed, the variation law of temperature and pressure field with depth is the same as the law previously mentioned. Figure 8 illustrates the process of obtaining the formation speed of hydrate in deep-water gas wells under various tool running speed conditions while maintaining other conditions constant and adjusting temperature and pressure point under the appropriate working conditions. The law that states that hydrate formation rate first increases slowly and then decreases rapidly with increasing depth also governs the relationship between hydrate formation rate and deep water. The rate at which hydrate forms in the reactor is not greatly affected by changes in lowering speed, i.e., hydrate formation in deep-water gas wells is not greatly affected by changes in tool lowering speed.

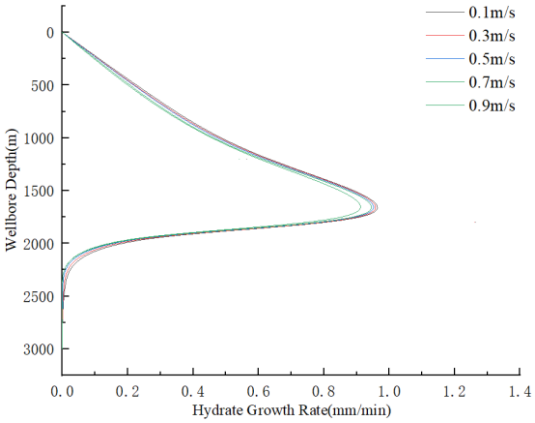

Figure 8. Variation diagram of hydrate formation rate under different release rates.

5. Conclusion

(1) A prediction model of deep-water high temperature and high-pressure wellbore temperature field is established, and the disturbance term of intervention operation is introduced for correction. This model is based on the wellbore structure of deep-water gas wells, taking into account the characteristics of intervention operations, combined with fluid heat conduction and convective heat transfer in the wellbore. To create a wellbore pressure prediction model for deep-water gas wells, the fluid friction factor in the wellbore under intervention operation is introduced, and the acceleration factor that causes the change of the fluid flow field is taken into account. The temperature and pressure model are solved iteratively to achieve the prediction of wellbore temperature and pressure during intervention operations.

(2) In this study, the three factors of gas production, running tool size, and running speed of deep-water gas wells are used to calculate the temperature and pressure curves under various conditions. It has been discovered that as the depth of a deep-water gas well decreases, the pressure gradually drops along with it, and as the depth decreases, the temperature gradually rises to that of seawater. Deep-water gas wells will experience a decrease in temperature and an increase in pressure as a result of increased gas production and larger running tools. The most significant changes in wellhead pressure and temperature at the mud line are caused by variations in gas production. Changes in

tool running speed have little impact on wellbore temperature and pressure, and wellbore temperature and pressure are less sensitive to changes in tool running speed.

(3) The rate of hydrate formation in the wellbore first rises and then falls as the depth of the well increases, peaking at a depth of about 1800 m, and then rapidly falling at a depth of 2000 m below the mud line. The production of deep-water gas wells and the size of the running tool both have a significant impact on the rate of hydrate formation, while the speed of the running tool has less of an impact. As the output of deep-water gas wells rises, the rate of hydrate formation decreases while the rate of hydrate formation rises as tool size increases. The maximum generation rate is reached when the running tool size percentage is 50%, and as the running tool size in the wellbore increases, the rate of hydrate formation decreases. In other words, the rate of hydrate generation in deep-water gas wells is not sensitive to the tool running rate. The influence of different running tool sizes has little bearing on the rate of hydrate generation in the wellbore.

References

[1] Wang ZY, Zhang JB, Meng WB, etc. Gas hydrate formation, deposition characteristics and control methods in deep-water gas wells. Chinese Journal of Petroleum. 2021;42(6):776-90. (in Chinese)
[2] Liu W, Sun Z, Hu J , et al. Prediction of Hydrate Formation Risk Based on Temperature-Pressure Field Coupling in the Deepwater Gas Well Cleanup Process. Energy & Fuels. 2021;35(3).
[3] Yu T, Guan G, Abudula A. Production performance and numerical investigation of the 2017 offshore methane hydrate production test in the Nankai Trough of Japan. Applied Energy, 2019, 251.
[4] Wang ZY, Sun BJ, Wang XR, et al. Prediction of natural gas hydrate formation region in wellbore during deep-water gas well testing. Hydrodynamics Research and Development Series B. 2014;26(4):568-576.
[5] Ma S, Huang J, Zhang F, et al. Prediction and Prevention of Hydrate Forming in Deep Water Gas Well Test. Journal of Xi'an Shiyou University(Natural Science Edition). 2017.
[6] Ren G, Zhang C, Dong Z, et al. Hydrate Deposition Performance in the Test String of Deep Water Gas Well. Special Oil & Gas Reservoirs. 2019.
[7] Yang JJ, Pu CS. A theoretical model of gas hydrate formation and blockage prediction in gas gathering pipelines. Natural Gas Geoscience. 2004;15(6):4. (in Chinese)
[8] Chang H. Prediction and Prevention of Hydrate Formation during Valve Action. China University of Petroleum, 2015. (in Chinese)
[9] Straume EO, Kakitani C, Merino-Garcia D, et al. Experimental Study of the Formation and Deposition of Gas Hydrates in Non-Emulsifying Oil and Condensate Systems. Chemical Engineering Science, 2016, 155:111-126.
[10] Song GC, Li YX, Wang WC, et al. Investigation of hydrate plugging in natural gas+diesel oil+water systems using a high-pressure flow loop. Chemical Engineeringence. 2017;158:480-89.
[11] Wang ZY, Zhang YY, Zhang JB, Tong SK, Sun BJ. Research progress on formation mechanism and prevention methods of hydrate flow obstacles in deep-water gas wells. China Science Foundation. 2021;35(06):992-1005. (in Chinese)
[12] Zhang JB. Mechanism and Law Analysis of Gas Hydrate Deposition and Blockage under the Condition of Controlled Annular Fog Flow in Deep-Water Wells. China University of Petroleum. 2018. (in Chinese)